Structure of the glassy fast-ion conductor $AgPS_3$ by neutron diffraction

Philip S. Salmon and Shuqin Xin
School of Physics, University of East Anglia, Norwich, NR4 7TJ, United Kingdom

Henry E. Fischer
Institut Laue-Langevin, Avenue des Martyrs, B.P. 156, F-38042 Grenoble Cedex 9, France

(Received 18 February 1998; revised manuscript received 13 May 1998)

The structure of the glassy fast-ion conductor g-$AgPS_3$ is studied by using the method of isotopic substitution in neutron diffraction. The diffraction pattern measured in a single experiment is separated into its contributions from the partial structure factor $S_{AgAg}(k)$, and related difference functions $\Delta_{Ag\mu}(k)$ and $\Delta_{\mu\mu}(k)$ comprising the Ag-μ and μ-μ correlations, respectively, where μ denotes a matrix atom (P or S) and k the scattering vector. It is found that the glass structure is significantly different from that of the corresponding crystalline compound c-$AgPS_3$. The $P_2S_6^{2-}$ units of the crystal are broken up to form tetrahedral PS_4 motifs with a P-S bond distance of 2.04(2) Å which are linked to form a matrix having pronounced intermediate-range order. The data for g-$AgPS_3$ are consistent with a model wherein the silver ions, coordinated to an average of 2.5(2) S at a bond distance of 2.53(2) Å, move via pathways which have a large distribution of Ag-Ag sites: in real space the Ag-Ag correlations are characterized by a broad ''liquidlike'' distribution with a nearest-neighbor distance of 2.9(1) Å and coordination number of 1.1(2). [S0163-1829(98)07334-2]

I. INTRODUCTION

A prerequisite for making progress in understanding the fundamental reasons for the existence of fast-ion conductivity in glassy materials is definitive structural information at the microscopic level: nonphenomenological approaches require detailed knowledge of the atomic positions to test models for interatomic forces. One of the main experimental challenges is, therefore, to measure the full set of (Faber-Ziman) partial structure factors $S_{\alpha\beta}(k)$ over a wide range of values of scattering vector k such that information is provided on both the short- and intermediate-range atomic ordering in real space. This task is particularly difficult owing to the inherent structural disorder of glassy materials and the presence of at least three different chemical species. However, for glasses of the type M-A-X, where M denotes a metal atom such as Cu or Ag, A denotes a group IVA or VA element, and X a chalcogen (S, Se, Te), considerable progress has recently been made. Specifically, when the atomic fraction of M is sufficiently high it is possible to separate the total structure factor $F(k)$, which is measured in a single diffraction experiment and comprises six $S_{\alpha\beta}(k)$, into the metal-metal partial structure factor $S_{MM}(k)$ and the difference functions $\Delta_{M\mu}(k)$ and $\Delta_{\mu\mu}(k)$ where μ denotes a matrix (A or X) atom and the latter two functions have contributions from the remaining two $S_{M\mu}(k)$ and three $S_{\mu\mu}(k)$, respectively.[1–3]

The rationale behind the study of M-A-X glasses stems from the fact that when a large mole fraction of a network modifier such as M_2X, which is a joint fast-ionic–electronic conductor in its high-temperature crystalline phase,[4–6] is mixed with a semiconducting network former such as A_2X_3 or AX, the resultant glasses sometimes become fast-ion conducting with M^+ ions as the mobile species.[7] In these circumstances the glasses become candidates for solid-state electrolytes in battery and sensor applications.[8,9] Results at the level of $S_{MM}(k)$ and related difference functions have been provided for the fast-ion conducting glass g-$(Ag_2Se)_{0.25}(AsSe)_{0.75}$ (Ref. 1) and the semiconducting glasses g-$(Ag_2Te)_{0.5}(As_2Te_3)_{0.5}$ (Ref. 2) and g-$(Cu_2Se)_{0.25}(AsSe)_{0.75}$ (Ref. 1). It is found that, irrespective of the mechanism for electrical conduction, the short-range order of the network former is not destroyed on mixing with a large mole fraction of network modifier and, at least for the Ag-based glasses, that elements of the intermediate-range order for the network modifier are retained. Furthermore, a broad ''liquidlike'' distribution of Ag-Ag nearest neighbors is observed for the fast-ion conductor whereas the distribution of M-M nearest neigbors for the semiconducting M-A-X glasses is much sharper. These observations suggest that the absence of ionic conductivity arises from a local trapping of the metal atom in the potential well of its nearest neighbors.[2] A broad distribution of Ag-Ag correlations was also found from neutron diffraction experiments on the fast-ion conductors g-$(Ag_2Se)_2(GeSe_2)_3Se$ (Ref. 10) and g-$(Ag_2S)_{0.5}(GeS_2)_{0.5}$ (Ref. 11) and the essential features of the short-range order for the network former are again retained.

The question naturally arises as to the generality of these results for other M-A-X glasses. In this context the glass g-$AgPS_3$, which occurs at $x=0.5$ on the pseudobinary tie line $(Ag_2S)_x(P_2S_5)_{1-x}$ $(0\leqslant x\leqslant 1)$, is an interesting candidate for study on several accounts.

(i) The compound involves a change in pnictogen from As to P and, unlike the other glasses previously studied at the level of $S_{MM}(k)$ and related difference functions, the matrix atom compound P_2S_5 does not appear to form a glass[12] and cannot therefore be regarded as a network former.

(ii) By contrast with the other M-A-X glasses for which $S_{MM}(k)$ and related difference functions have been measured, a crystalline compound having the same stoichiometry as the glass can be formed. The structure of c-$AgPS_3$ has

been measured[13] and therefore provides an excellent basis for comparison with the neutron diffraction results for the glass. Furthermore, several other crystalline systems exist on the $(Ag_2S)_x(P_2S_5)_{1-x}$ pseudobinary tie line, viz., two modifications of c-$Ag_4P_2S_7$ ($x=0.67$) (Refs. 14 and 15), c-$Ag_7P_3S_{11}$ ($x=0.7$) (Ref. 16), c-Ag_3PS_4 ($x=0.75$) (Ref. 15), and two modifications of c-Ag_7PS_6 ($x=0.875$) (Ref. 15) although most occur outside the glass-forming region of $0.33 \leqslant x \leqslant 0.67$.[17–19] Two modifications of c-$Ag_4P_2S_6$ also occur and their structures have been measured.[20,21]

(iii) The electrical conductivity of g-$AgPS_3$ is reported to be between 7.8×10^{-7} Ω^{-1} cm^{-1} (Ref. 19) and $\approx 7\times10^{-6}$ Ω^{-1} cm^{-1} (Ref. 17) at 25 °C and the transport number is 0.99,[17] which implies that conduction proceeds by the movement of Ag^+ ions. By contrast c-$AgPS_3$ is predominantly an electronic conductor of very low total conductivity, viz., 3.2×10^{-9} Ω^{-1} cm^{-1} at 25 °C.[19]

(iv) The short-range order of $(Ag_2S)_x(P_2S_5)_{1-x}$ glasses has been studied by ^{31}P magic-angle spinning nuclear magnetic resonance (NMR) and dipolar NMR techniques by Zhang *et al.*[18] It was concluded that the addition of Ag_2S to P_2S_5 introduces nonbridging sulphur atoms, resulting in a continuous network transformation, and that phosphorus-phosphorus bonds are absent for the entire glass-forming region. The $P_2S_6^{2-}$ groups of c-$AgPS_3$ do not exist in the glassy phase to any appreciable extent but are broken up to form PS_4^- units. Information on the μ-μ correlations is therefore available for comparison with the neutron diffraction results.

In this paper the essential theory required to understand the diffraction results will first be given. The sample preparation and characterization together with the neutron diffraction experimental method will then be outlined. Next, the neutron diffraction results for g-$AgPS_3$ will be presented and the procedure required to extract $S_{MM}(k)$ and related difference functions will be explained. Finally the results will be discussed and a brief comparison made with the structures of other glassy *M-A-X* systems.

II. THEORETICAL BACKGROUND

A. Data correction procedure

In a reactor-based neutron diffraction experiment the total structure factor $F(k)$ for a glass comprising ν chemical species labeled α or β is extracted from the measured intensities by using the relations[22]

$$F_o(k) \equiv F(k) + \sum_{\alpha=1}^{\nu} c_\alpha [b_\alpha^2 + b_{inc,\alpha}^2][1+P_\alpha(k)] = \frac{1}{N_s A_{s,sc}(\theta)} \left\{ \left[\frac{I_{cs}(\theta)}{a(\theta)} - M_{cs}(\theta) \right] - \frac{A_{c,cs}(\theta)}{A_{c,c}(\theta)} \left[\frac{I_c(\theta)}{a(\theta)} - M_c(\theta) \right] \right\}, \quad (1)$$

where $F_o(k)$ represents the observed differential cross section for coherent and incoherent scattering, $F(k)$ is expressed by

$$F(k) = \sum_{\alpha=1}^{\nu} \sum_{\beta=1}^{\nu} c_\alpha c_\beta b_\alpha b_\beta [S_{\alpha\beta}(k) - 1], \quad (2)$$

and $a(\theta)$ is a normalization factor measured by reference to a vanadium standard.[23] The atomic fraction, bound coherent scattering length, and bound incoherent scattering length of chemical species α are denoted by c_α, b_α, and $b_{inc,\alpha}$, respectively, and the scattering vector k is related to the incident neutron wavelength λ and scattering angle 2θ through $k = 4\pi\lambda^{-1}\sin\theta$. The $P_\alpha(k)$ arise from inelasticity effects and are usually calculated by using a Placzek expansion,[24] N_s represents the number of illuminated sample atoms, and $A_{i,j}(\theta)$ denotes a Paalman-Pings[25] attenuation factor which refers to neutrons that are scattered in medium i and attenuated, through absorption and scattering, in medium j. The intensities $I_{cs}(\theta)$ and $I_c(\theta)$ for the sample (s) in its container (c) and for the empty container, respectively, are corrected for background scattering by reference to a Cd absorber at low 2θ values.[26] The $M_i(\theta)$ are the multiple scattering cross sections calculated in the quasi-isotropic approximation using the method of Soper and Egelstaff.[27] The correction procedure given by Eq. (1) ensures that the attenuation corrections are applied to once-scattered neutrons.

B. Difference functions

By making diffraction experiments on three *M-A-X* glasses which are identical in every respect, except for the isotopic composition of M, three total structure factors $F(k)$, $'F(k)$, and $''F(k)$ are measured corresponding to scattering lengths $b_M > b_{'M} > b_{''M}$. Those correlations not involving a metal atom can then be extracted by subtracting two total structure factors to give a first-order difference function, e.g.,

$$\Delta_M^{(1)}(k) \equiv F(k) - {}''F(k) = \Delta_{M\mu}^{(1)}(k) + c_M^2 \delta_M^{(1)} \mathfrak{s}_M^{(1)} [S_{MM}(k) - 1], \quad (3)$$

where $\delta_M^{(1)} = b_M - b_{''M}$, $\mathfrak{s}_M^{(1)} = b_M + b_{''M}$, and

$$\Delta_{M\mu}^{(1)}(k) = 2c_M c_A b_A \delta_M^{(1)} [S_{MA}(k) - 1] + 2c_M c_X b_X \delta_M^{(1)} \times [S_{MX}(k) - 1]. \quad (4)$$

The other first-order difference functions are defined by $\Delta_M^{(2)}(k) \equiv F(k) - {}'F(k)$ and $\Delta_M^{(3)}(k) \equiv {}'F(k) - {}''F(k)$. It is then possible to eliminate the M-μ correlations by using, for example, the combination[28,29]

$$\Delta F^{(1)}(k) \equiv F(k) - b_M \Delta_M^{(1)}(k)/\delta_M^{(1)} = {}''F(k) - b_{''M}\Delta_M^{(1)}(k)/\delta_M^{(1)} = [b_M {}''F(k) - b_{''M} F(k)]/\delta_M^{(1)} = \Delta_{\mu\mu}^{(1)}(k) - c_M^2 b_M b_{''M} [S_{MM}(k) - 1], \quad (5)$$

where

$$\Delta_{\mu\mu}^{(1)}(k) = c_A^2 b_A^2 [S_{AA}(k) - 1] + c_X^2 b_X^2 [S_{XX}(k) - 1] + 2c_A c_X b_A b_X [S_{AX}(k) - 1]. \quad (6)$$

Similarly $\Delta F^{(2)}(k) \equiv F(k) - b_M \Delta_M^{(2)}(k)/\delta_M^{(2)} = {}'F(k) - b_{'M} \Delta_M^{(2)}(k)/\delta_M^{(2)}$, where $\delta_M^{(2)} = b_M - b_{'M}$ and $\Delta F^{(3)}(k) \equiv {}'F(k) - b_{'M} \Delta_M^{(3)}(k)/\delta_M^{(3)} = {}''F(k) - b_{''M} \Delta_M^{(3)}(k)/\delta_M^{(3)}$, where $\delta_M^{(3)} = b_{'M} - b_{''M}$. Equations (3) and (5) are particularly useful if only two structure factors are measured in an experiment.[28] However, the measurement of three total structure factors enables $S_{MM}(k)$ to be extracted through the second-order difference function[1,29]

$$\begin{aligned} S_{MM}(k) - 1 &= [\Delta_M^{(2)}(k) - \gamma \Delta_M^{(1)}(k)][c_M^2 \gamma(1-\gamma)(\delta_M^{(1)})^2]^{-1} \\ &= [(1-\gamma)F(k) - {}'F(k) + \gamma {}''F(k)] \\ &\quad \times [c_M^2 \gamma(1-\gamma)(\delta_M^{(1)})^2]^{-1}, \end{aligned} \tag{7}$$

where $\gamma = \delta_M^{(2)}/\delta_M^{(1)}$ and $(1-\gamma) = \delta_M^{(3)}/\delta_M^{(1)}$ with $0 < \gamma < 1$. The M-μ correlations can then be isolated by the elimination of $S_{MM}(k)$ from Eq. (3) to give Eq. (4) which may be written, in terms of the total structure factors, as

$$\begin{aligned} \Delta_{M\mu}^{(1)}(k) &= [-(\mathfrak{s}_M^{(1)} - \gamma \mathfrak{s}_M^{(2)})F(k) + \mathfrak{s}_M^{(1)\prime} F(k) - \gamma \mathfrak{s}_M^{(2)\prime\prime} F(k)] \\ &\quad \times [\gamma(1-\gamma)\delta_M^{(1)}]^{-1}, \end{aligned} \tag{8}$$

where $\mathfrak{s}_M^{(2)} = b_M + b_{'M}$. The remaining functions $\Delta_{M\mu}^{(2)}(k)$ and $\Delta_{M\mu}^{(3)}(k)$ follow from similar expressions such that $\Delta_{M\mu}^{(1)}(k)/\delta_M^{(1)} = \Delta_{M\mu}^{(2)}(k)/\delta_M^{(2)} = \Delta_{M\mu}^{(3)}(k)/\delta_M^{(3)}$. The μ-μ correlations can also be isolated by the elimination of $S_{MM}(k)$ from Eq. (5) to give Eq. (6) which may be written, in terms of the total structure factors, as

$$\begin{aligned} \Delta_{\mu\mu}^{(1)}(k) &= [(1-\gamma) b_{'M} b_{''M} F(k) - b_M b_{''M} {}'F(k) \\ &\quad + \gamma b_M b_{'M} {}''F(k)][\gamma(1-\gamma)(\delta_M^{(1)})^2]^{-1}. \end{aligned} \tag{9}$$

Likewise, $\Delta_{\mu\mu}^{(2)}(k)$ and $\Delta_{\mu\mu}^{(3)}(k)$ follow from the elimination of $S_{MM}(k)$ from $\Delta F^{(2)}(k)$ and $\Delta F^{(3)}(k)$, respectively, and, in theory, all three $\Delta_{\mu\mu}^{(i)}(k)$ $(i=1,2,3)$ are identical. Hence the total structure factors can be written as, e.g.,

$$F(k) = \Delta_{\mu\mu}^{(1)}(k) + \frac{b_M}{\delta_M^{(1)}} \Delta_{M\mu}^{(1)}(k) + c_M^2 b_M^2 [S_{MM}(k) - 1], \tag{10}$$

which emphasizes their separation into a linear combination of the μ-μ, M-μ, and M-M correlation functions.

Fourier transformation of the total structure factors $F(k)$, ${}'F(k)$, and ${}''F(k)$ gives the real-space functions $G(r)$, ${}'G(r)$, and ${}''G(r)$, respectively. The relevant expressions are obtained from Eq. (2) by replacing the $S_{\alpha\beta}(k)$ by the partial pair distribution functions $g_{\alpha\beta}(r)$. The r-space representations of the difference functions $\Delta_M^{(i)}(k)$, $\Delta_{M\mu}^{(i)}(k)$, $\Delta F^{(i)}(k)$, and $\Delta_{\mu\mu}^{(i)}(k)$ $(i=1,2,3)$ are denoted by $\Delta G_M^{(i)}(r)$, $\Delta G_{M\mu}^{(i)}(r)$, $\Delta G^{(i)}(r)$, and $\Delta G_{\mu\mu}^{(i)}(r)$, respectively, and are obtained from the above equations for the k-space functions by again replacing the $S_{\alpha\beta}(k)$ by the $g_{\alpha\beta}(r)$. The mean coordination number of β around α is denoted by $\overline{n}_\alpha^\beta$.

C. Systematic errors and self-consistency checks

An important property of the difference functions represented by Eqs. (3), (7), and (8) is that the coefficients of the total structure factors sum to zero. The inelasticity corrections $P_\alpha(k)$ for chemical species that are not isotopically substituted will therefore cancel [see Eq. (1)], and it can be shown that the inelasticity corrections for the isotopically substituted species are often considerably reduced.[30] Furthermore, provided that the same container is used for all sample measurements and that the total absorption and scattering cross sections of the samples are similar, the multiple scattering and container corrections in Eq. (1) will themselves be similar for all samples. Hence the use of Eqs. (3), (7), and (8) will lead to a cancellation, to first order, of any systematic errors that may arise from these corrections. These arguments do not hold for Eqs. (5) and (9) as the coefficients of the total structure factors do not sum to zero. However, the effect of any systematic errors on these difference functions will often be small because the $\Delta_{\mu\mu}^{(i)}(k)$ $(i=1,2,3)$, which dominate the $\Delta F^{(i)}(k)$ $(i=1,2,3)$ [Eq. (5)], generally make a large contribution to the measured total structure factors as found from consideration of Eq. (10).

The efficacy of the data correction procedure, and hence the reliability of the measured k-space functions, can be tested on several accounts since the functions must tend to the correct high-k limit, obey the usual sum rule relations,[31] and produce well-behaved r-space functions: the back-Fourier-transform obtained after setting the unphysical low-r oscillations to their calculated limit should be in good overall agreement with the original k-space function.[29] Furthermore, the measured $\Delta_{\mu\mu}^{(i)}(k)$ $(i=1,2,3)$ should be the same within the statistical uncertainties as should the $\Delta_{M\mu}^{(i)}(k)/\delta_M^{(i)}$ $(i=1,2,3)$.

III. EXPERIMENTAL METHOD

A. Glass preparation and characterization

Three samples $^{107}AgPS_3$, $^{109}AgPS_3$, and $^{N}AgPS_3$, where N denotes the natural isotopic abundance of Ag, were prepared under identical conditions using a procedure designed to avoid sample contamination.[32,33] Elemental ^{N}Ag (99.999% Aldrich), ^{107}Ag (98.53% enrichment), or ^{109}Ag (98.56% enrichment) was mixed with elemental phosphorus (99.999% Aldrich) and sulphur (99.999% JMC Specpure) within silica ampoules (1 mm wall thickness, 5 mm internal diameter) held in a rocking furnace, and the glasses were made by quenching the ampoules from 600 °C in an ice–salt-water mixture at −5 °C. The isotopic compositions were chosen to maximize the overall silver scattering length contrast to ensure that $\gamma \approx 0.5$ in Eq. (7). The samples were characterized by using a TA Instruments Thermal Analyst 2000 differential scanning calorimeter at a heating rate of 10 °C min^{-1}. Glass transition temperatures of 192(3) °C (onset) and 202(3) °C (midpoint) were measured for all three samples, in excellent agreement with the results of Zhang *et al.*[18,19] An endothermic event starting at 452(3) °C and of enthalpy 104(3) J g^{-1} was recorded and may be identified with decomposition of the material.[15] A density of 3.54 g cm^{-3}, corresponding to $n_0 = 0.0454$ Å^{-3}, was measured for g-$^{N}AgPS_3$ by using a volumetric flask and solvents of various densities. This value compares with 3.35 g cm^{-3} as measured by Kawamoto and Nishida[17] and 3.68 g cm^{-3} for c-$AgPS_3$[13].

TABLE I. Weighting factors for the $S_{\alpha\beta}(k)$ (in mbarn) for g-$AgPS_3$.

	$S_{AgAg}(k)$	$S_{AgP}(k)$	$S_{AgS}(k)$	$S_{PP}(k)$	$S_{SS}(k)$	$S_{PS}(k)$
$^{107}F(k)$	22.53(7)	30.80(8)	51.28(8)	10.53(4)	29.18(2)	35.05(7)
$^{N}F(k)$	14.03(3)	24.30(6)	40.46(5)	10.53(4)	29.18(2)	35.05(7)
$^{109}F(k)$	7.10(4)	17.29(6)	28.79(8)	10.53(4)	29.18(2)	35.05(7)
$\Delta^{(1)}_{Ag}(k)$	15.43(8)	13.51(10)	22.49(11)	-	-	-
$\Delta^{(2)}_{Ag}(k)$	8.50(8)	6.50(10)	10.82(9)	-	-	-
$\Delta^{(3)}_{Ag}(k)$	6.93(5)	7.01(8)	11.67(9)	-	-	-
$\Delta^{(1)}_{Ag\mu}(k)$	-	13.51(10)	22.49(11)	-	-	-
$\Delta F^{(1)}(k)$	-12.65(4)	-	-	10.53(4)	29.18(2)	35.05(7)
$\Delta F^{(2)}(k)$	-17.78(3)	-	-	10.53(4)	29.18(2)	35.05(7)
$\Delta F^{(3)}(k)$	-9.98(3)	-	-	10.53(4)	29.18(2)	35.05(7)
$\Delta^{(1)}_{\mu\mu}(k)$	-	-	-	10.53(4)	29.18(2)	35.05(7)

B. Neutron diffraction experiments

The neutron diffraction experiments were made at room temperature (ca. 23 °C) using the instrument D4B at the Institut Laue-Langevin, Grenoble. The incident neutron wavelength of 0.7034 Å ensured measurement of the diffraction patterns over a wide k-space range, $0.25 \leqslant k(\text{Å}^{-1}) \leqslant 16.2$. The glasses were in the form of coarsely ground lumps and were held in a cylindrical thin-walled (0.1 mm) vanadium container of internal diameter 6.8 mm. The scattering length values are $b(^{107}\text{Ag}) = 7.505(11)$ fm, $b(^{N}\text{Ag}) = 5.922(7)$ fm, $b(^{109}\text{Ag}) = 4.214(11)$ fm, $b_P = 5.13(1)$ fm, and $b_S = 2.847(1)$ fm.[34] The weighting factors for the $S_{\alpha\beta}(k)$ appearing in the various formulas are given in Table I and $\Delta^{(1)}_{Ag\mu}(k) = 2.08\Delta^{(2)}_{Ag\mu}(k) = 1.93\Delta^{(3)}_{Ag\mu}(k)$ while $\Delta^{(1)}_{\mu\mu}(k) = \Delta^{(2)}_{\mu\mu}(k) = \Delta^{(3)}_{\mu\mu}(k)$.

IV. RESULTS

A. Total structure factors

It was found that the total structure factors first produced by using Eq. (1) had small but definite slopes which were similar in magnitude for each function (Fig. 1). The shape of these slopes was found to be consistent with a small degree of hydrogen contamination in keeping with the extremely hygroscopic nature of the glassy samples[18] and a need to store them for three years prior to their use in the neutron diffraction experiments. Since the *incoherent* scattering cross section of hydrogen is very much greater than the coherent scattering cross sections of the other chemical species in the glass,[34] the predominant effect of the water contamination will be to alter the self-scattering terms involving the $b_{inc,\alpha}$ in Eq. (1) while making little change to $F(k)$. The effective differential cross section for the incoherent scattering by hydrogen was calculated by using the procedure given by Salmon and Lond[35] and was subtracted from the original total structure factors to give the fully corrected functions illustrated in Fig. 1. The amount of hydrogen in each sample was estimated to be small at between 1.2 and 2.2 mol. %. Good agreement is found between $^{N}F(k)$ and $^{N}\tilde{F}(k)$, the back-Fourier-transform obtained after setting the unphysical low-r oscillations in $^{N}G(r)$ to their calculated limit $^{N}G(0)$, which shows that the slope caused by water contamination has been successfully eliminated at the total structure factor level. Good agreement is also found between $^{107}F(k)$ and $^{107}\tilde{F}(k)$ and between $^{109}F(k)$ and $^{109}\tilde{F}(k)$. A first sharp diffraction peak (FSDP), which is a signature of intermediate-range atomic ordering,[36] is observed in all three total structure factors at 1.17(3) Å^{-1}.

B. Difference functions

1. Ag-Ag correlations

$S_{AgAg}(k)$ was extracted by using Eq. (7) with the total structure factors represented by the error bars in Fig. 1. It was found that the resultant function had a noticeable droop at high k which indicates that the hydrogen correction described in Sec. IV A is not sufficiently accurate at the second-order difference function level. However, it proved possible to refine this correction by substituting the total structure factors for their back-Fourier-transforms $^{107}\tilde{F}(k)$, $^{N}\tilde{F}(k)$, and $^{109}\tilde{F}(k)$, represented by the solid

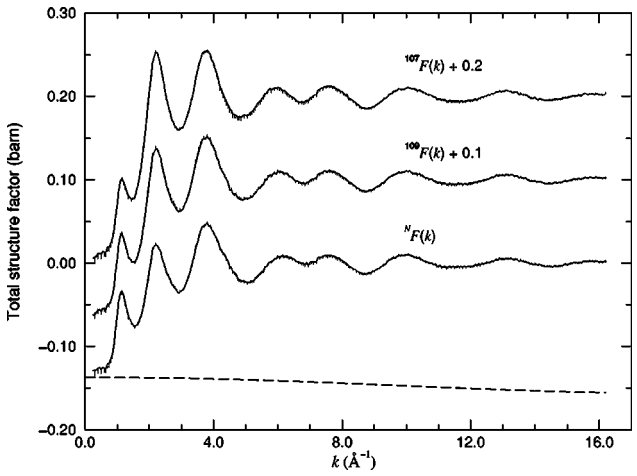

FIG. 1. The measured total structure factors for g-$AgPS_3$ corrected for the effect of hydrogen contamination. The bars represent the statistical error on a data point and the solid curves are the back-Fourier-transforms [(e.g., $^{N}\tilde{F}(k)$] of the corresponding real-space functions [(e.g., $^{N}G(r)$] after their unphysical low-r oscillations are set to the calculated limiting value [(e.g., $^{N}G(0)$]. The dashed curve shows the effective differential cross section for hydrogen which was used to correct $^{N}F(k)$ (see Sec. IV A).

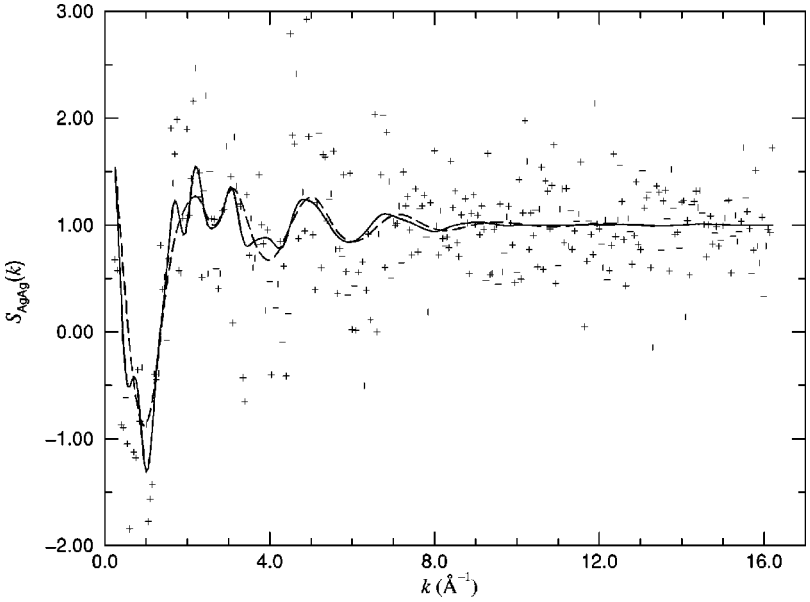

FIG. 2. $S_{\mathrm{AgAg}}(k)$ for g-$AgPS_3$. The crosses are obtained by using Eq. (7) with the total structure factors shown as the solid curves in Fig. 1. The dashed curve is the result obtained after spline fitting the measured data to reduce the effect of statistical noise and corresponds to the dashed curve in Fig. 3. The solid curve is the MIN solution and corresponds to the solid curve in Fig. 3.

curves in Fig. 1. No discernible droop could be observed on the resultant Ag-Ag partial structure factor which is shown in Fig. 2.

Next, $g_{\mathrm{AgAg}}(r)$ was obtained by using three methods, namely, (a) by Fourier transforming $S_{\mathrm{AgAg}}(k)$ represented by the data points in Fig. 2, (b) by Fourier transforming a spline fit to the data points in order to reduce the effect of statistical noise, and (c) by using the the minimum noise (MIN) reconstruction method of Soper *et al.*[37] This method gives, essentially, a smoother function wherein the $g_{\alpha\beta}(r)$ are constrained to take physical values, i.e., $g_{\alpha\beta}(r)=0$ for $0\leqslant r \leqslant r_{min}$ and $g_{\alpha\beta}(r)\geqslant 0$ for $r\geqslant r_{min}$. Neither of the functions produced by Fourier transformation gave a peak at the position of the first peak in either $\Delta G^{(i)}_{\mathrm{Ag}}(r)$ or $\Delta G^{(i)}(r)(i=1,2,3)$ which indicates that there are no unwanted Ag-μ or μ-μ correlations. The robustness of $S_{\mathrm{AgAg}}(k)$ was tested by adjusting the weighting factors on the total structure factors in Eq. (7) within their calculated errors. No significant change in $g_{\mathrm{AgAg}}(r)$ was noted. The r-space functions obtained by all three methods give comparable peak positions and coordination numbers, i.e., $r_1=3.01(2)$ Å, $r_2=3.82(2)$ Å, and $\overline{n}^{\mathrm{Ag}}_{\mathrm{Ag}}=1.1(2)$ from method (a), $r_1=2.82(2)$ Å, $r_2=4.16(2)$ Å, and $\overline{n}^{\mathrm{Ag}}_{\mathrm{Ag}}=1.1(2)$ from method (b), and $r_1=2.96(2)$ Å, $r_2=3.98(2)$ Å, and $\overline{n}^{\mathrm{Ag}}_{\mathrm{Ag}}=1.0(2)$ from method (c), where r_1 and r_2 denote the first and second peak positions, respectively. The $g_{\mathrm{AgAg}}(r)$ obtained from the latter two methods are shown in Fig. 3.

2. Ag-matrix atom correlations

The $\Delta^{(i)}_{\mathrm{Ag}\mu}(k)(i=1,2,3)$ are shown in Fig. 4 and were extracted from the first-order difference functions by using Eq. (3) with $S_{\mathrm{AgAg}}(k)$ taken from the dashed curve in Fig. 2. The differences $[\Delta^{(1)}_{\mathrm{Ag}\mu}(k)-2.08\Delta^{(2)}_{\mathrm{Ag}\mu}(k)]$ and $[\Delta^{(1)}_{\mathrm{Ag}\mu}(k)-1.93\Delta^{(3)}_{\mathrm{Ag}\mu}(k)]$ have no obvious structure which shows, from the discussion in Sec. II C, that the data analysis has been properly undertaken. The $\Delta^{(i)}_{\mathrm{Ag}\mu}(k)$ have a broad FSDP at 0.92(3) Å^{-1}, indicating the presence of intermediate-range atomic ordering associated with one or both of the contributing partial structure factors $S_{\mathrm{AgS}}(k)$ and $S_{\mathrm{AgP}}(k)$. The MIN method was used to produce $\Delta G^{(1)}_{\mathrm{Ag}\mu}(r)$ and the result is shown in Fig. 5.

In c-$AgPS_3$ silver is coordinated to four different hexathiodimetaphosphate $P_2S_6{}^{2-}$ ions via Ag-S bonds of length 2.66 Å.[13] Each silver atom has two nearest-neighbor nonbonding phosphorus atoms within the $P_2S_6{}^{2-}$ ions at 3.63 Å and another two at 3.66 Å. On the basis of this crystal structure the first peak in $\Delta G^{(1)}_{\mathrm{Ag}\mu}(r)$ at 2.53(2) Å, which covers the range $2.33\leqslant r(\text{Å})\leqslant 2.95$, can be assigned to Ag-S correlations and its integration gives $\overline{n}^{\mathrm{S}}_{\mathrm{Ag}}=2.5(2)$. Similarly, the second peak in $\Delta G^{(1)}_{\mathrm{Ag}\mu}(r)$ at 3.57(3) Å will have a contribution from both Ag-P and Ag-S correlations while the third peak at 5.52(4) Å will be dominated by Ag-S correlations (see Fig. 5).

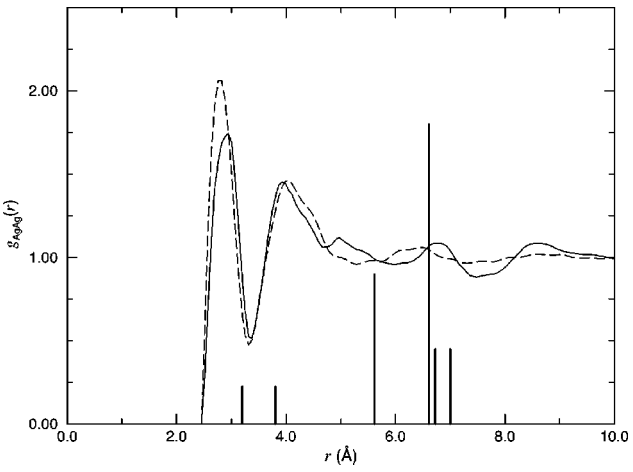

FIG. 3. $g_{\mathrm{AgAg}}(r)$ for g-$AgPS_3$. The dashed curve was obtained by Fourier transforming a spline fit to $S_{\mathrm{AgAg}}(k)$ and corresponds to the dashed curve in Fig. 2. The solid curve is the MIN solution and corresponds to the solid curve in Fig. 2. The vertical bars mark the positions of the Ag-Ag correlations in c-$AgPS_3$ (Ref. 13) and their heights are proportional to the coordination numbers with $\overline{n}^{\mathrm{Ag}}_{\mathrm{Ag}}=1$ for the first nearest neighbors.

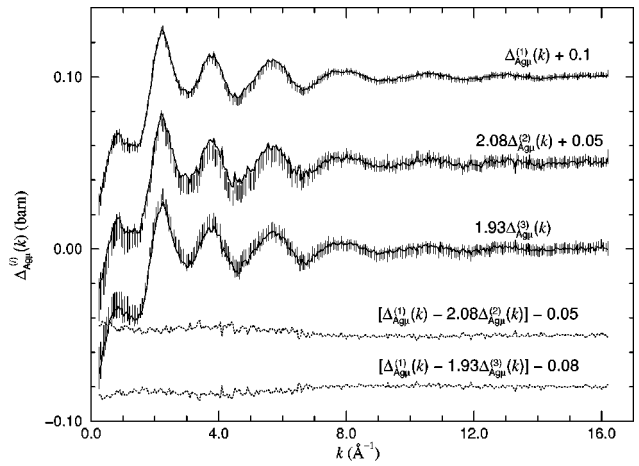

FIG. 4. The Ag-matrix atom difference functions $\Delta^{(i)}_{\mathrm{Ag}\mu}(k)$ $(i=1,2,3)$ for g-$AgPS_3$. The bars represent the statistical error on a measured data point and the solid curves are the back-Fourier-transforms of the corresponding $\Delta G^{(i)}_{\mathrm{Ag}\mu}(r)$ after their unphysical low-r oscillations are set to the calculated $\Delta G^{(i)}_{\mathrm{Ag}\mu}(0)$ limit. The differences between the scaled $\Delta^{(i)}_{\mathrm{Ag}\mu}(k)$ functions are also shown.

3. Matrix-matrix atom correlations

The $\Delta^{(i)}_{\mu\mu}(k)(i=1,2,3)$ are shown in Fig. 6 and were extracted from the $\Delta F^{(i)}(k)$ by using Eq. (5) with $S_{\mathrm{AgAg}}(k)$ taken from the dashed curve in Fig. 2. The differences $[\Delta^{(1)}_{\mu\mu}(k)-\Delta^{(2)}_{\mu\mu}(k)]$ and $[\Delta^{(1)}_{\mu\mu}(k)-\Delta^{(3)}_{\mu\mu}(k)]$ have no obvious structure which implies, from the discussion in Sec. II C, that the functions are free from any substantial systematic error. They have a strong FSDP at 1.16(2) Å^{-1} which indicates a high degree of matrix-atom intermediate-range ordering of periodicity $2\pi/k_{FSDP}=5.42$ Å.[36] The MIN method was used to produce $\Delta G^{(1)}_{\mu\mu}(r)$ and the result is shown in Fig. 7.

In c-$AgPS_3$ the matrix atoms form hexathiodimetaphosphate $P_2S_6^{2-}$ ions in which the two P atoms are linked by two S bridging atoms to give a short P-P distance of 2.90 Å.[13] Each phosphorus atom is surrounded by four sulphur atoms in a highly distorted tetrahedral arrangement with a P-S bond length of 2.00–2.12 Å and only S-S correlations are found in the range $3.37\leqslant r(\text{Å})\leqslant 3.74$ for which $\overline{n^{\mathrm{S}}_{\mathrm{S}}}=7.3$. No evidence of phosphorus-phosphorus bonds was found from the NMR experiments of Zhang *et al.*[18] for any of the glasses formed along the $(Ag_2S)_x(P_2S_5)_{1-x}$ pseudobinary tie line. The first peak in $\Delta G^{(1)}_{\mu\mu}(r)$ at 2.04(2) Å is therefore attributed to P-S bonds and, with this assignment, its integration over the range $1.84\leqslant r(\text{Å})\leqslant 2.33$ gives a coordination number $\overline{n^{\mathrm{S}}_{\mathrm{P}}}=4.1(2)$. The broad but low-intensity feature in $\Delta G^{(1)}_{\mu\mu}(r)$ for $2.33\leqslant r(\text{Å})\leqslant 3.07$ will include nonbonded P-P correlations and the second peak at 3.36(2) Å will be dominated by nonbonded S-S correlations. However, integration of this latter feature over the range $3.07\leqslant r(\text{Å})\leqslant 3.74$ gives $\overline{n^{\mathrm{S}}_{\mathrm{S}}}=5.2(4)$; i.e., the $P_2S_6^{2-}$ structural motifs of c-$AgPS_3$ are broken up in the glassy phase. The ratio of the first and second peak positions is 1.647 which is close to the ratio $\sqrt{8/3}=1.633$ expected for perfect tetrahedral coordination and suggests that the coordination environment of phosphorus is more regular than in c-$AgPS_3$.

It is also interesting to compare the structure of g-$AgPS_3$ with that of c-P_2S_5 since the glass lies at $x=0.5$ on the $(Ag_2S)_x(P_2S_5)_{1-x}$ pseudobinary tie line. Crystalline c-P_2S_5 comprises cagelike P_4S_{10} molecular units in which each phosphorus atom is tetrahedrally bonded to four sulphur atoms with one P-S double bond of length 1.91 – 1.98 Å and three P-S single bonds of length 2.02 – 2.13 Å.[38–40] In the P_4S_{10} molecule, coordination numbers of $\overline{n^{\mathrm{P}}_{\mathrm{P}}}=3$ and $\overline{n^{\mathrm{S}}_{\mathrm{S}}}=4.6$ are obtained for the ranges $3.37\leqslant r(\text{Å})\leqslant 3.44$ and $3.24\leqslant r(\text{Å})\leqslant 3.46$, respectively. However, integration of the second peak in $\Delta G^{(1)}_{\mu\mu}(r)$ (Fig. 7) over the range $3.07\leqslant r(\text{Å})\leqslant 3.74$ and assuming $\overline{n^{\mathrm{P}}_{\mathrm{P}}}=3$ gives $\overline{n^{\mathrm{S}}_{\mathrm{S}}}=2.0(2)$; i.e., there is no evidence from the data to support the existence of P_4S_{10} molecules in g-$AgPS_3$.

V. DISCUSSION

A. Ag-Ag correlations

The nearest-neighbor Ag-Ag distance of 2.9(1) Å in g-$AgPS_3$ is comparable to the values of 3.2 Å found in both

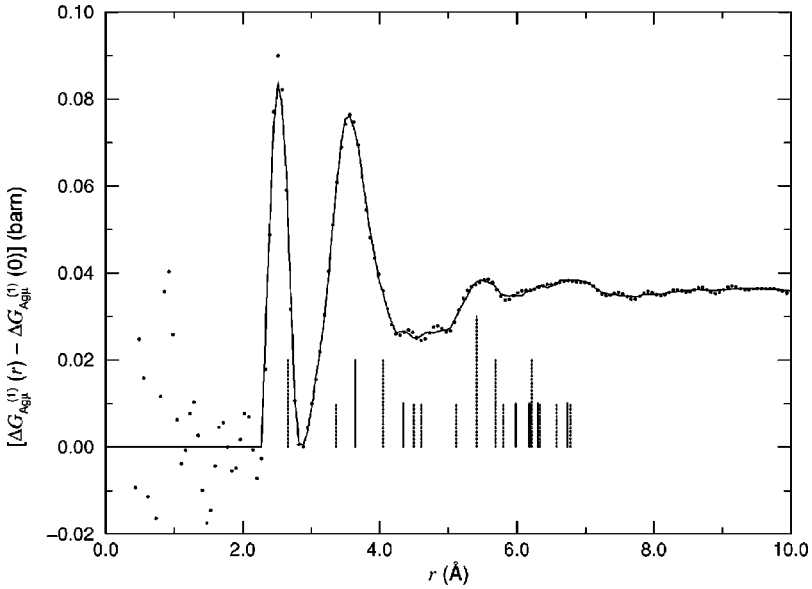

FIG. 5. $[\Delta G^{(1)}_{\mathrm{Ag}\mu}(r)-\Delta G^{(1)}_{\mathrm{Ag}\mu}(0)]$ $=22.49g_{\mathrm{AgS}}(r)+13.51g_{\mathrm{AgP}}(r)$ (in mbarn) for g-$AgPS_3$. The solid circles are obtained by Fourier transforming $\Delta^{(1)}_{\mathrm{Ag}\mu}(k)$ given by the error bars in Fig. 4 and the solid curve is the MIN solution. The vertical bars mark the positions of the Ag-S (dashed line) and Ag-P (solid line) correlations in c-$AgPS_3$ (Ref. 13) and their heights are proportional to the coordination numbers with $\overline{n^{\mathrm{S}}_{\mathrm{Ag}}}=\overline{n^{\mathrm{P}}_{\mathrm{Ag}}}=4$ for the first nearest neighbors.

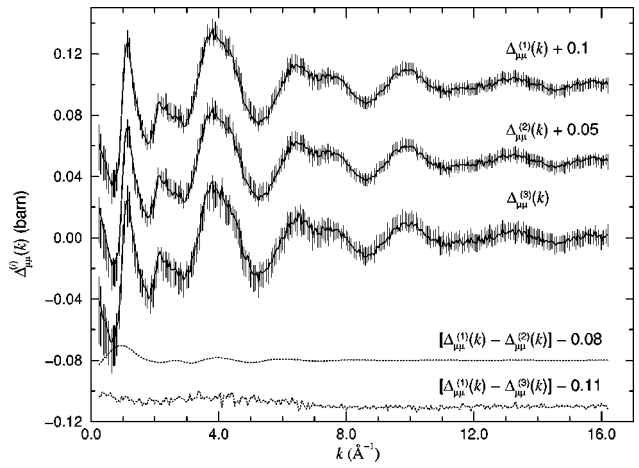

FIG. 6. The matrix-matrix atom difference functions $\Delta_{\mu\mu}^{(i)}(k)$ $(i=1,2,3)$ for g-$AgPS_3$. The bars represent the statistical error on a measured data point and the solid curves are the back-Fourier-transforms of the corresponding $\Delta G_{\mu\mu}^{(i)}(r)$ after the unphysical low-r oscillations are set to their calculated $\Delta G_{\mu\mu}^{(i)}(0)$ limit. The differences between the measured $\Delta_{\mu\mu}^{(i)}(k)$ functions are also shown.

c-$AgPS_3$[13] and c-$Ag_4P_2S_6$ (Ref. 20) and 3.1 Å found in the fast-ion phase of c-Ag_2S.[41,42] This observation of nearest-neighbor Ag-Ag distances that are relatively short when compared with those in crystalline Ag (2.89 Å) is a characteristic feature of the structural chemistry of several Ag(I) compounds[43] and is independent of whether the glass is a fast-ion conductor or semiconductor.[1–3,11] The Ag-Ag distance is, however, longer than the observed Ag-S distance of 2.53(2) Å and it is unclear as to whether there exists bonded or nonbonded Ag-Ag interactions.

The first peak in $g_{\mathrm{AgAg}}(r)$ is fairly broad, in the sense that it does not return to the $g_{\mathrm{AgAg}}(0)$ limit on its high-r side, as are the remaining peaks shown in Fig. 3. These features are typical of the partial pair distribution functions of the mobile species for liquids such as CuCl,[44] CuBr,[45,46] NiI_2,[47] and Ag_2Se,[6] which melt from a fast-ion crystalline phase. The second and third peaks in $g_{\mathrm{AgAg}}(r)$ for g-$AgPS_3$ [i.e., g-$(Ag_2S)_{0.5}(P_2S_5)_{0.5}$] at $r_2=4.0(2)$ Å and $r_3=6.7(2)$ Å do not occur at positions comparable to those found in the high-temperature fast-ion phase of c-Ag_2S by anomalous x-ray scattering experiments [$r_2=5.6(2)$ Å] (Ref. 41) or by molecular dynamics calculations [$r_2=5.0(2)$ Å, $r_3=8.0(2)$ Å] (Ref. 42). The intermediate-range atomic ordering associated with c-Ag_2S is therefore broken up when it is mixed with 50 mol % of P_2S_5 to form g-$AgPS_3$. This observation contrasts with that for the glassy fast-ion conductor g-$(Ag_2Se)_{0.25}(AsSe)_{0.75}$ (Ref. 1) and semiconductor g-$(Ag_2Te)_{0.5}(As_2Te_3)_{0.5}$ (Ref. 2) because the first five peaks in the measured $g_{\mathrm{AgAg}}(r)$ for these glasses occur at positions that are comparable to those found in the high-temperature fast-ion phases of c-Ag_2Se and c-Ag_2Te, respectively.

As shown in Fig. 3, the maxima in $g_{\mathrm{AgAg}}(r)$ for g-$AgPS_3$ occur at different positions to the Ag-Ag distances in c-$AgPS_3$ (Ref. 13) and the Ag-Ag correlations in the glassy phase are characterized by a much greater distribution of distances. This latter observation resembles the situation found in the crystalline ionic conductor c-$Ag_7P_3S_{11}$ where the Ag^+ ions are disordered amoung the interstices in the anion array formed by layers of PS_4^{3-} groups which alternate with double layers of $P_2S_7^{4-}$ groups.[16,19]

B. Ag-μ correlations

The nearest-neighbor Ag-μ correlations in the glass are significantly different to those in c-$AgPS_3$ (Ref. 13) where Ag forms a distorted tetrahedron with the S atoms of four different $P_2S_6^{2-}$ ions wherein the Ag-S distance is 2.66 Å. The Ag-S distance of 2.53(2) Å in the glass is much smaller than the sum of ionic radii for Ag^+ (1.26 Å) and S^{2-} (1.84 Å) (Ref. 48) which is indicative of substantial covalent character for the Ag-S interaction.[49] This is consistent with the low value of $\overline{n}_{\mathrm{Ag}}^{\mathrm{S}}=2.5(2)$ which may be interpreted in terms of the glass comprising equal numbers of twofold and threefold coordinated silver atoms. In crystalline fast-ion conductors it is argued[50,51] that the potential barrier to ionic motion between sites is lowered in the case of Ag(I) and Cu(I) compounds owing to the ability of these cations to exist in a variety of low-coordination-number environments. Low $\overline{n}_M^X$ coordination numbers of $\approx 3-4$ are also a feature of many

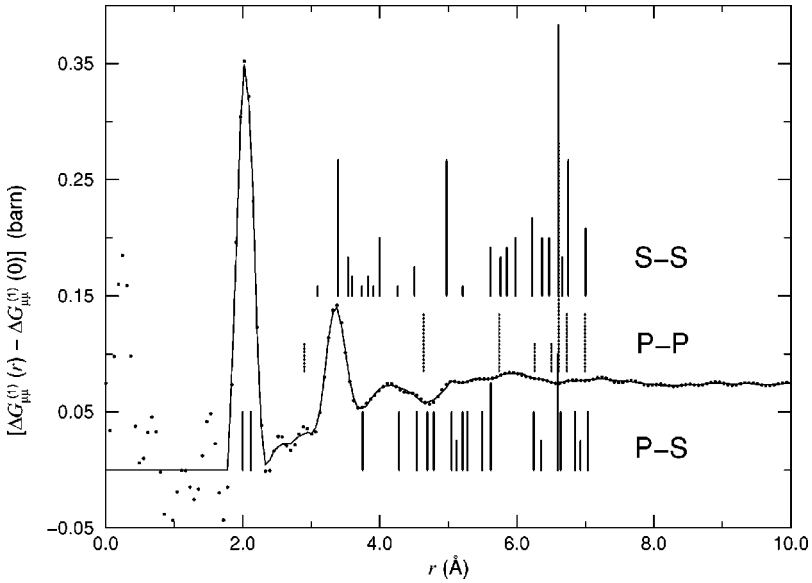

FIG. 7. $[\Delta G_{\mu\mu}^{(1)}(r)-\Delta G_{\mu\mu}^{(1)}(0)]=35.05g_{\mathrm{PS}}(r)+10.53g_{\mathrm{PP}}(r)+29.18g_{\mathrm{SS}}(r)$ (in mbarn) for g-$AgPS_3$. The solid circles are obtained by Fourier transforming $\Delta_{\mu\mu}^{(1)}(k)$ given by the error bars in Fig. 6 and the solid curve is the MIN solution. The vertical bars mark the positions of the P-S, P-P and S-S correlations in c-$AgPS_3$ (Ref. 13) and their heights are proportional to the coordination numbers with $\overline{n}_{\mathrm{P}}^{\mathrm{S}}=2$, $\overline{n}_{\mathrm{P}}^{\mathrm{P}}=1$, and $\overline{n}_{\mathrm{S}}^{\mathrm{S}}=0.33$ for the first nearest neighbors.

other *M-A-X* glasses but there is no clear correlation between the precise value of $\overline{n}_M^X$ and whether the glass is a fast-ion conductor or a semiconductor.[3]

The results for g-$AgPS_3$ are inconsistent with the model of Kastner[52] which predicts that group I metal atoms will be fourfold coordinated by the chalcogen when the covalent component to the bonding is significant and electronic d states are not involved. It appears, therefore, that d states are important and the relative stability of threefold versus fourfold coordination for Ag(I) compounds has been investigated by Burdett and Eisenstein[53] using an orbital approach. It is argued that the lower-coordination-number conformation can be stabilized over the regular tetrahedral arrangement if there is a distortion via a second-order Jahn-Teller effect wherein the d orbitals of the occupied outer shell are mixed with the s orbitals of the valence shell.

C. μ-μ correlations

The diffraction data for g-$AgPS_3$ show tetrahedral coordination of P by S and that the $P_2S_6^{2-}$ structural motifs of c-$AgPS_3$ are broken up in the glassy phase. These observations are consistent with the NMR results of Zhang *et al.*[18] who concluded that the $P_2S_6^{2-}$ groups of c-$AgPS_3$ do not exist in the glassy phase to any significant extent but are disrupted to form PS_4^- units.

There is no evidence to support destruction of the *short*-range order of the matrix atom compound c-P_2S_5 when it is mixed with a large mole fraction of c-Ag_2S to form g-$AgPS_3$. Similarly, in g-$(Ag_2Se)_{0.25}(AsSe)_{0.75}$,[1] g-$(Ag_2Te)_{0.5}(As_2Te_3)_{0.5}$,[2] and g-$(Cu_2Se)_{0.25}(AsSe)_{0.75}$,[1], the short-range order of the network-forming compound is not destroyed. However, g-$AgPS_3$ is characterized by a larger degree of intermediate-range atomic ordering with respect to the fact that, while a FSDP is a prominent feature in $\Delta G_{\mu\mu}^{(1)}(r)$ for g-$AgPS_3$, no such feature is observed in $\Delta G_{\mu\mu}^{(1)}(r)$ for these other glasses. It is interesting to speculate whether this observation arises from the ability of phosphorus to form tetrahedral motifs.

VI. CONCLUSIONS

The structure of g-$AgPS_3$ is found to be significantly different from that of the corresponding crystalline compound. The $P_2S_6^{2-}$ units of the crystal are broken up to form tetrahedral PS_4 structural motifs which are linked to form a matrix having pronounced intermediate-range order. The data are consistent with a model wherein the silver ions move between sites in which they have a low mean coordination number of $\overline{n}_{Ag}^S = 2.5(2)$ via pathways which have a large distribution of Ag-Ag sites.

ACKNOWLEDGMENTS

It is a pleasure to thank Dr. Jian Liu for making the glassy samples and Jonathan Wasse and Dr. C. E. Anson for providing detailed information on the structure of c-$AgPS_3$. S.X. wishes to thank the University of East Anglia and the CVCP for support. P.S.S. wishes to thank The Queen's College, Oxford for support during the tenure of which this work was completed and the hospitality of Professor Paul A. Madden and the PTCL. The financial support of the UK EPSRC is gratefully acknowledged.

[1] C. J. Benmore and P. S. Salmon, Phys. Rev. Lett. **73**, 264 (1994).
[2] J. Liu and P. S. Salmon, Europhys. Lett. **39**, 521 (1997).
[3] P. S. Salmon and J. Liu, J. Non-Cryst. Solids **205-207**, 172 (1996).
[4] K. Shahi, Phys. Status Solidi A **41**, 11 (1977).
[5] J. B. Boyce and B. A. Huberman, Phys. Rep. **51**, 189 (1979).
[6] A. C. Barnes, S. B. Lague, P. S. Salmon, and H. E. Fischer, J. Phys.: Condens. Matter **9**, 6159 (1997).
[7] Z. U. Borisova, *Glassy Semiconductors* (Plenum, New York, 1981).
[8] A. Feltz, *Amorphous Inorganic Materials and Glasses* (VCH, Weinheim, 1993).
[9] E. Bychkov, Sens. Actuators B **26-27**, 351 (1995).
[10] R. J. Dejus, S. Susman, K. J. Volin, D. G. Montague, and D. L. Price, J. Non-Cryst. Solids **143**, 162 (1992).
[11] J. H. Lee, A. P. Owens, A. Pradel, A. C. Hannon, M. Ribes, and S. R. Elliott, Phys. Rev. B **54**, 3895 (1996).
[12] Y. Monteil and H. Vincent, Z. Anorg. Allg. Chem. **428**, 259 (1977).
[13] P. Toffoli, P. Khodadad, and N. Rodier, Acta Crystallogr., Sect. B: Struct. Crystallogr. Cryst. Chem. **34**, 3561 (1978).
[14] P. Toffoli, P. Khodadad, and N. Rodier, Acta Crystallogr., Sect. B: Struct. Crystallogr. Cryst. Chem. **33**, 1492 (1977).
[15] H. Andrae and R. Blachnik, J. Therm. Anal. **35**, 595 (1989).
[16] P. Toffoli, P. Khodadad, and N. Rodier, Acta Crystallogr., Sect. B: Struct. Crystallogr. Cryst. Chem. **38**, 2374 (1982).
[17] Y. Kawamoto and M. Nishida, J. Non-Cryst. Solids **20**, 393 (1976).
[18] Z. Zhang, J. H. Kennedy, and H. Eckert, J. Am. Chem. Soc. **114**, 5775 (1992).
[19] Z. Zhang and J. H. Kennedy, J. Electrochem. Soc. **140**, 2384 (1993).
[20] P. Toffoli, A. Michelet, P. Khodadad, and N. Rodier, Acta Crystallogr., Sect. B: Struct. Crystallogr. Cryst. Chem. **38**, 706 (1982).
[21] P. Toffoli, P. Khodadad, and N. Rodier, Acta Crystallogr., Sect. C: Cryst. Struct. Commun. **39**, 1485 (1983).
[22] P. S. Salmon, J. Phys. F **18**, 2345 (1988).
[23] D. M. North, J. E. Enderby, and P. A. Egelstaff, J. Phys. C **1**, 784 (1968).
[24] J. L. Yarnell, M. J. Katz, R. G. Wenzel, and S. H. Koenig, Phys. Rev. A **7**, 2130 (1973).
[25] H. H. Paalman and C. J. Pings, J. Appl. Phys. **33**, 2635 (1962).
[26] H. Bertagnolli, P. Chieux, and M. D. Zeidler, Mol. Phys. **32**, 759 (1976).
[27] A. K. Soper and P. A. Egelstaff, Nucl. Instrum. Methods **178**, 415 (1980).
[28] I. T. Penfold and P. S. Salmon, Phys. Rev. Lett. **64**, 2164 (1990).
[29] P. S. Salmon and C. J. Benmore, in *Recent Developments in the Physics of Fluids*, edited by W. S. Howells and A. K. Soper

(Hilger, Bristol, 1992), p. F225.
[30] A. K. Soper, G. W. Neilson, J. E. Enderby, and R. A. Howe, J. Phys. C **10**, 1793 (1977).
[31] J. E. Enderby, D. M. North, and P. A. Egelstaff, Philos. Mag. **14**, 961 (1966).
[32] I. T. Penfold and P. S. Salmon, J. Non-Cryst. Solids **114**, 82 (1989).
[33] S. Xin, Ph.D. thesis, University of East Anglia, 1996.
[34] V. F. Sears, Neutron News **3**, 26 (1992).
[35] P. S. Salmon and P. B. Lond, J. Phys.: Condens. Matter **4**, 5249 (1992).
[36] P. S. Salmon, Proc. R. Soc. London, Ser. A **445**, 351 (1994).
[37] A. K. Soper, C. Andreani, and M. Nardone, Phys. Rev. E **47**, 2598 (1993).
[38] A. Vos and E. H. Wiebenga, Acta Crystallogr. **8**, 217 (1955).
[39] M. Gardner, J. Chem. Soc. Dalton Trans. **1973**, 691.
[40] M. Somer, W. Bues, and W. Brockner, Z. Naturforsch. A **38**, 163 (1983).
[41] Y. Tsuchiya, S. Tamaki, Y. Waseda, and J. M. Toguri, J. Phys. C **11**, 651 (1978).
[42] P. Vashishta, I. Ebbsjö, R. Dejus, and K. Sköld, J. Phys. C **18**, L291 (1985).
[43] A. F. Wells, *Structural Inorganic Chemistry* (Clarendon Press, Oxford, 1984).
[44] S. Eisenberg, J.-F. Jal, J. Dupuy, P. Chieux, and W. Knoll, Philos. Mag. A **46**, 195 (1982).
[45] D. A. Allen and R. A. Howe, J. Phys.: Condens. Matter **4**, 6029 (1992).
[46] L. Pusztai and R. L. McGreevy, J. Phys.: Condens. Matter **10**, 525 (1998).
[47] N. D. Wood, R. A. Howe, R. J. Newport, and J. Faber, Jr., J. Phys. C **21**, 669 (1988).
[48] *CRC Handbook of Chemistry and Physics*, 67th ed., edited by R. C. Weast (CRC, Boca Raton, 1986), p. F157.
[49] J. E. Enderby and A. C. Barnes, Rep. Prog. Phys. **53**, 85 (1990).
[50] R. D. Armstrong, R. S. Bulmer, and T. Dickinson, J. Solid State Chem. **8**, 219 (1973).
[51] P. McGeehin and A. Hooper, J. Mater. Sci. **12**, 1 (1977).
[52] M. Kastner, Philos. Mag. B **37**, 127 (1978).
[53] J. K. Burdett and O. Eisenstein, Inorg. Chem. **31**, 1758 (1992).